Influence of the p-type doping on the radiometric performances of MWIR InAs/GaSb superlattice photodiodes

E. Giard, I. Ribet-Mohamed, M. Delmas, J.B. Rodriguez, P. Christol

▶ To cite this version:

HAL Id: hal-01070571

https://hal-onera.archives-ouvertes.fr/hal-01070571

Submitted on 1 Oct 2014

Influence of the p-type doping on the radiometric performances of MWIR InAs/GaSb superlattice photodiodes.

E. Giard[a]*, I. Ribet-Mohamed[a], M. Delmas[b,c], J.B. Rodriguez[b,c], P. Christol[b,c]

[a]*ONERA, Chemin de la Hunière, 91761 Palaiseau- France*

[b]*Univ. Montpellier, IES, UMR 5214, F- 34000, Montpellier, France*

[c]*CNRS, IES, UMR 5214, F- 34000, Montpellier, France*

Abstract

In this paper, quantum efficiency (QE) measurements performed on type-II InAs/GaSb superlattice (T2SL) photodiodes operating in the mid-wavelength infrared domain, are reported. Several comparisons were made in order to determine the SL structure showing optimum radiometric performances : same InAs-rich SL structure with different active zone thicknesses (from 0.5µm to 4µm) and different active zone doping (n-type versus p-type), same 1µm thick p-type active zone doping with different SL designs (InAs-rich versus GaSb-rich and symmetric SL structures). Best result was obtained for the p-type doped InAs-rich SL photodiode, with a 4µm active zone thickness, showing a QE that reaches 61% at $\lambda = 2$µm and 0V bias voltage.

[*]Corresponding author: Tel.: (+33) 180 386 334;
                              e-mail address: edouard.giard@onera.fr

1. Introduction

Type II InAs/GaSb superlattices (T2SL) were introduced in the early 70s by Esaki and Tsu [1]. T2SL mid-wavelength infrared (MWIR) pin photodiodes were first studied by Yang and Bennet in 1994 [2]. Since then, significant improvements were obtained on SL detectors as show demonstrations of high-performance MWIR focal plane arrays (FPA) [3-7]. These performances were obtained with devices designed with barriers [8-10] to reduce the generation recombination dark current. Another way to enhance performances is to reduce the Shockley-Read-Hall (SRH) recombination mechanism in order to increase the carrier lifetimes. Most T2SL devices exhibit shorter carrier lifetime than InAs/InAsSb superlattices [11]. But InAs/InAsSb superlattices have not yet reached the same performance than T2SL in terms of quantum efficiency (QE) and dark current [12].

Therefore to combine the long carrier lifetime of the InAs/InAsSb superlattice and the good QE of the T2SL, an InAs-rich T2SL was proposed [13]: this superlattice exhibits an InAs to GaSb thickness ratio close to R=2. Good performances in terms of dark current were already reported [13-15] but a recent study tends to prove a problem of minority carrier collection with this design [16] leading to non-optimal performances in terms of QE.

In this paper, we report on quantum efficiency of MWIR SL photodiodes with active zone made of asymmetric period composed of 7 InAs monolayers (MLs) / 4 GaSb MLs (7/4 SL structure), showing cut-off wavelength at 5µm (77K). We study the influence of a p-type doping in the active zone in order to correct the non-optimal collection of the minority carriers. Then we study the influence of the InAs to GaSb thickness ratio on the radiometric performances of MWIR InAs/GaSb superlattice photodiodes.

2. Samples

The InAs/GaSb SL structure for the MWIR domain was grown on p-type GaSb substrate by Molecular Beam Epitaxy. The growth procedure, the epitaxy characterization and the device processing were already reported [14]. The structure is described in Fig. 1: it consists of a 200 nm Be-doped (p+ type doping $\sim 1 \times 10^{18} cm^{-3}$) GaSb buffer layer, a 60nm Be-doped (p+ type doping $\sim 1 \times 10^{18} cm^{-3}$) SL layer, an InAs/GaSb SL active zone, a 60nm Te-doped (n+ type doping $\sim 1 \times 10^{18} cm^{-3}$) SL layer, and a 20 nm Te-doped (n+-type doping $\sim 1 \times 10^{18} cm^{-3}$) InAs cap layer. Different samples are presented in this paper: the first samples (A, B, C) have an InAs-rich design with active layer thickness varying from 500nm (155 periods) to 4μm (1240 periods). The asymmetric period of this non-intentionally doped (nid) active zone is composed of 7 InAs monolayers (MLs) / 4 GaSb MLs (7/4 SL structure). Then the second set of samples contains two InAs-rich (7/4 SL structure) samples (D, E) with active layer thickness of 500nm and 4μm respectively. But, unlike the first set of samples, the active zone of these samples is Be-doped (p type doping $\sim 1 \times 10^{15} cm^{-3}$). The two last samples exhibit an active layer thickness equal to 1μm with two different designs: sample F is a GaSb-rich (10/19) SL structure and sample B a symmetric (10/10) SL structure. These samples are listed in Table 1.

All these samples exhibit photoluminescence emission and cut-off wavelength around 5μm at 77K. From epitaxial SL material, circular mesa photodiodes were fabricated using standard photolithography. The devices were placed in a LN_2 bath cryostat ready to perform photoelectrical measurements at 77K. All measurements presented below were performed with a front side illumination (through the InAs cap layer) on 160μm diameter photodiodes.

3

3. Influence of the active zone thickness on the QE spectrum for InAs-rich T2SL pin photodiodes

To investigate an eventual non-optimal collection of the minority carriers suspected [16] in the InAs-rich SL structure, we decided to measure QE spectra of several InAs-rich samples with different active zone thicknesses (AZT). Fig. 2 presents the QE spectra of three InAs-rich samples with different nid AZT: 500nm (sample A), 1µm (sample B) and 4µm (sample C). The QE spectra were measured at 77K and 0V bias voltage.

Each QE spectrum was measured in two steps. First the relative photoresponse was measured using a FTIR spectrometer and then the absolute QE was calibrated using a SR200 blackbody [16].

The following comments can be made on Fig. 2: at 0V bias voltage, the QE between λ = 4.5µm and λ = 5µm doesn't depend on the thickness of the active layer. However, at 0V bias voltage for shorter wavelengths, the thinner the active zone is, the higher the QE is. In the inset of Fig. 2 are plotted the experimental QE of the same samples at λ = 4.5µm versus the electric field, calculated as the ratio between the bias voltage and the active zone thickness. The QE of the thinnest active zone presents no bias voltage dependence. The QE of the 1µm thick active zone increases with the reverse bias voltage until -10 000V/cm (U_{bias} = -1V), and is constant for high reverse bias voltages. The QE of the thickest active zone increases linearly also with the reverse bias voltage. This reverse bias dependence of the QE could be the signature of a non-optimal minority carrier collection. Indeed, the nid region of the InAs-rich SL structures is expected to be n-type residual at 77K, therefore the minority carriers are the holes. The real P-N junction is between the active layer and the p+-doped SL layer, "far" from the illuminated side which is the InAs cap layer. The space charge region (SCR) width was calculated with the Poisson's equations equal to 451nm for 0V bias voltage. The 500nm thick active zone is quite completely depleted at 0V whereas the 1µm thick active zone and the 4µm

4

thick active zone are not. Therefore, the bias dependence of the QE (see the inset of Fig. 2) and the low QE values at 0V bias voltage for short wavelengths and thick structures (see Fig. 2) can be explained by a short hole diffusion length. The hole diffusion length is necessarily shorter than 500nm because the 1μm thick active zone is not completely depleted at 0V and the QE of this device increases linearly until -10 000V/cm.

4. Influence of the p-type doping on the QE spectrum of InAs-rich T2SL photodiodes.

To optimize the minority carrier collection, we decided to dope the active zone with Beryllium (p- type doping $\sim 5 \times 10^{15} cm^{-3}$). Be-doping was already used to increase the performances of InAs-rich structure but only in the long-wavelength infrared (LWIR) domain [17]. In the Be-doped active zone, the minority carriers are the electrons, unlike in the nid active zone in which the minority carriers are the holes (n-type residual doping). Because the electron mobility is higher than the hole mobility, the electron diffusion length is expected to be longer than the hole diffusion length.

Fig. 3 presents the QE spectrum of sample D at 0V bias voltage and 77K operating temperature. Sample D has a p- doped active zone and its active zone thickness is equal to 4μm. Sample D was compared to sample C which has the same active zone thickness and the same 7/4 design but its active zone is nid. The QE of p doped active zone is higher than the QE of the nid active zone in the entire spectrum. The QE reaches 61% at $\lambda = 2\mu m$. In the p doped active zone, nearly all photo-generated carriers are collected, whereas, in the nid active zone, carriers which are photo-generated far from the SCR are not collected. The inset of Fig. 3 presents the experimental QE of samples C and D at $\lambda = 4.5\mu m$ versus the bias voltage. For reverse bias voltages higher than -0.4V, the QE of sample D is nearly constant. It means that the electron diffusion length is long enough to collect nearly all minority carriers. But it also

5

means that the electron diffusion length is shorter than 4µm because between 0V and -0.4V the QE increases with the reverse bias voltage.

5. Influence of the SL design on the QE spectrum of T2SL photodiodes.

To study the influence of the InAs to GaSb thickness ratio on the radiometric performances of MWIR InAs/GaSb superlattice photodiodes, two other samples were grown with different designs: sample F exhibits a GaSb-rich design (10/19 SL structure) and sample G exhibits a symmetric design (10/10 SL structure). These two samples have a 1µm thick active layer. Therefore we can compare these samples with sample B but not with sample D which is thicker.

That's why we decided to interpolate the QE spectrum of a 1µm thick p-doped active zone. We used the Hovel's expression [18] where the total QE is the sum of three contributions:

$$QE = \text{QE}_{SCR} + QE_n + QE_p \qquad (1)$$

where QE_{SCR} is the contribution of the space charge region, QE_n is the contribution from the quasineutral n region and QE_p is the contribution from the quasineutral p region. The contribution from the quasineutral n region is negligible because that layer is thin and has a low hole mobility therefore $\text{QE}_n \approx 0$.

$$\text{QE}_{SCR} = (1 - R) \times (e^{-\alpha x_n} - e^{-\alpha x_p}) \qquad (2)$$

$$\text{QE}_p = (1 - R)\frac{\alpha L_n}{(\alpha L_n)^2 - 1}e^{-\alpha x_p}(\alpha L_n - \frac{\sinh\left(\frac{W}{L_n}\right) + \alpha L_n e^{-\alpha W}}{\cosh\left(\frac{W}{L_n}\right)}) \qquad (3)$$

where R is the reflectivity of the top surface, α is the absorption coefficient, x_n and x_p are the n and p depletion regions, W is the SCR width and L_n is the electron diffusion length. α is proportional to the density of states. A realistic hypothesis for the InAs-rich structure is a quasi 3D density of states owing to the large electron-holes wave-function overlap [14]. Therefore α was taken proportional to the square root of the energy.

6

Only the shape of the curve was simulated by these equations: therefore to simplify the model, the surface recombination velocity was set equal to zero. Then the relative magnitudes were calibrated using the experimental data of samples D and E. Sample E has a 500nm thick p-doped active zone. Fig. 4 presents the calibration of the simulated QE for these two samples and the interpolation of the QE for a 1µm thick p-doped active zone. This interpolation was also reported in Fig. 5 where a comparison between this simulated p-doped InAs-rich spectrum and three experimental QE spectra (samples B, F, G) of T2SL photodiodes with 1µm thick active zone was made. The three samples present different design: sample F is GaSb-rich, G is symmetric and B is InAs-rich and its active zone is n type residual. The last curve is the QE simulated for a p doped InAs-rich active zone. The p-doped InAs-rich active zone exhibits higher QE than the GaSb-rich and the symmetric active zones in the entire spectrum. This result confirms what was expected [13], that the InAs-rich design is more efficient than the symmetric and the GaSb designs. The absorption is better in the InAs-rich design because of its large electron-holes wave-function overlap.

6. Conclusion

QE were measured on T2SL test photodiodes, with different AZT or different SL designs, with or without Be-doping in the active zone. The highest QE at 0V bias voltage was obtained with an InAs-rich 7/4 SL structure with a p-type doped active zone. For this structure, with a 4µm thick active zone, the QE at 77K reaches 61% at $\lambda = 2$µm. This study highlights the influence of the p-type doping on the radiometric performances of T2SL detectors.

REFERENCES

[1] L. Esaki and R. Tsu. "Superlattice and negative differential conductivity in semiconductors," IBM Journal of Research and Development 14.1 (1970): 61-65.

[2] M.J. Yang, and B.R. Bennet "InAs/GaSb infrared photovoltaic detector at 77K," Electron. Lett. 30 (1994) 1710.

[3] E. Plis, M.N. Kutty, and S. Krishna "Review of passivation techniques for InAs/GaSb strained layer superlattice detectors", Laser & Photonics Reviews 7 (2011) 1.

[4] R. Rehm, M. Walther, J. Schmitz, J. Fleißner, F. Fuchs, J. Ziegler, W. Cabanski "InAs/GaSb superlattice focal plane arrays for high-resolution thermal imaging," Opto-Electron. Rev. 14 (2006) 19.

[5] J. W. Little, S. P. Svensson, W. A. Beck, A. C. Goldberg, S. W. Kennerly, T. Hongsmatip, M. Winn, and P. Uppal, "Thin active region, type II superlattice photodiode arrays : single-pixel and focal plane array characterization," J. Appl. Phys. 101 (2007) 044514.

[6] S.D. Gunapala, D.Z. Ting, C. J. Hill, J. Nguyen, A. Soibel, S. B. Rafol, S.A. Keo, J.M. Mumolo, M.C. Lee, J.K. Liu, B. Yang, and A. Liao, "Demonstration of 1Kx1K long-wave and mid-wave superlattice infrared focal plane arrays," Proc. SPIE 7808 (2010) 780802.

[7] E.K. Huang, S. A. Pour, M.A. Hoang, A. Haddadi, M. Razeghi, and M. Z. Tidrow, "Low irradiance background limited type-II superlattice MWIR M-barrier imager," Optics letters, Vol. 37, No. 11 (2012).

[8] J.-B. Rodriguez, E. Plis, G. Bishop, Y.D. Sharma, H. Kim, and S. Krishna, "nBn structure based on InAs/GaSb type-II strained layer superlattices," Appl. Phys. Lett. 91 (2007) 043514.

[9] B.-M. Nguyen, D. Hoffman, P.-Y. Delaunay and M. Razeghi. "Dark current suppression in type II InAs/GaSb superlattice long wavelength infrared photodiodes with M-structure barrier," Appl. Phys. Lett. 91 (2007) 163511.

[10] D.Z.Y. Ting, C.J. Hill, A. Soibel, S.A. Keo, J.M. Mumolo, J. Nguyen, and S.D. Gunapala, "A high-performance long wavelength superlattice complementary barrier infrared detector," Appl. Phys. Lett. 95 (2009) 023508.

[11] B.V. Olson, E.A. Shaner, J.K. Kim, J.F. Klem, S. D. Hawkins, L.M. Murray, J.P. Prineas, M.E. Flatte, and T.F. Boggess, "Time-resolved optical measurements of minority

carrier recombination in a mid-wave infrared InAsSb alloy and InAs/InAsSb superlattice," Appl. Phys. Lett. 101 (2012) 092109.

[12] T. Schuler-Sandy, S. Myers, B. Klein, N. Gautam, P. Ahirwar, Z.-B. Tian, T. Rotter, G. Balakrishnan, E. Plis, and S. Krishna, "Gallium free type II InAs/InAs$_x$Sb$_{1-x}$ superlattice photodetectors," Appl. Phys. Lett. 101 (2012) 071111.

[13] J.-B. Rodriguez, C. Cervera, and P. Christol, "A type-II superlattice period with a modified InAs to GaSb thickness ratio for midwavelength infrared photodiode performance improvement," Appl. Phys. Lett. 97 (2010) 251113.

[14] R. Taalat, J.-B. Rodriguez, M. Delmas, and P. Christol "Influence of the period thickness and composition on the electro-optical properties of type-II InAs/GaSb midwave infrared superlattice photodetectors," J. of Phys. D: Appl. Phys. 47.1 (2014) 015101.

[15] R. Taalat, J.-B. Rodriguez, C. Cervera, I. Ribet-Mohamed, and P. Christol, "Electrical characterizations of asymmetric InAs/GaSb superlattice MWIR photodiodes," Infrared Physics & Technology 59 (2013) 32-35.

[16] E. Giard, R. Taalat, M. Delmas, J-B. Rodriguez, P. Christol, and I. Ribet-Mohamed, "Radiometric and noise characteristics of InAs-rich T2SL MWIR pin photodiodes," Journal of the European Optical Society-Rapid publications 9 (2014).

[17] D. Hoffman, B.-M. Nguyen, P.-Y. Delaunay, A. Hood, M. Razeghi, and J. Pellegrino, "Beryllium compensation doping of InAs/GaSb infrared superlattice photodiodes," Applied Physics Letters 91 (2007) 143507-143507.

[18] J. Hovel, "Semiconductors and Semimetals", Academic, New York, Vol. 11 (1975) 17–20.

FIGURE CAPTIONS

Figure 1 : Schematic view of the SL structure on p-type GaSb substrate.

Figure 2 : Experimental QE spectra for InAs-rich SL photodiodes with different active zone thicknesses at 77K and 0V bias voltage (samples A, B, C with active thickness equal to 500nm, 1µm, 4µm, respectively). Inset: Experimental QE at $\lambda = 4.5$µm versus electric field for these InAs-rich SL photodiodes.

Figure 3 : Comparison between QE spectrum of InAs-rich SL photodiode with 4µm nid active zone and QE spectrum of InAs-rich SL photodiode with 4µm thick p-doped (5×10^{15}cm^{-3}) active zone (samples C, D respectively), at 77K and 0V bias voltage. Inset: Experimental QE at $\lambda = 4.5$µm versus bias voltage for these two SL photodiodes.

Figure 4 : Experimental (samples D and E) and simulated QE spectra of p-type doped InAs-rich photodiodes with different active zone thicknesses.

Figure 5 : Experimental and simulated QE spectra for three different T2SL designs with 1µm active zone thickness at 77K and 0V bias voltage.

TABLE CAPTIONS

Table 1 : SL photodiode sample characteristics.

TABLES

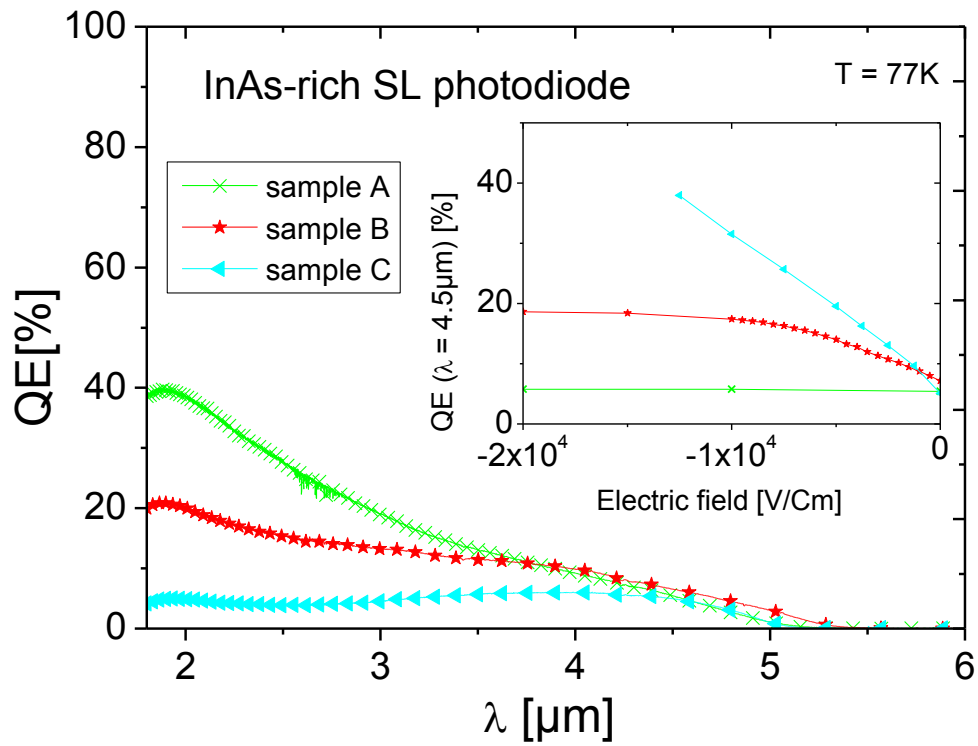| Sample	A	B	C	D	E	F	G
Design (ML InAs/ ML GaSb)	InAs-rich 7/4	InAs-rich 7/4	InAs-rich 7/4	InAs-rich 7/4	InAs-rich 7/4	GaSb-rich 10/19	Symmetric 10/10
Active zone doping	nid n residual	nid n residual	nid n residual	p-type	p-type	nid p residual	nid p residual
Active zone thickness	500nm	1µm	4µm	4µm	500nm	1µm	1µm

Table 1

E. Giard *et al.*

Influence of the p-type doping on the radiometric performances of MWIR InAs/GaSb

superlattice photodiodes

Figure 1

E. Giard *et al.*

Influence of the p-type doping on the radiometric performances of MWIR InAs/GaSb superlattice photodiodes

Figure 2

E. Giard *et al.*

Influence of the p-type doping on the radiometric performances of MWIR InAs/GaSb
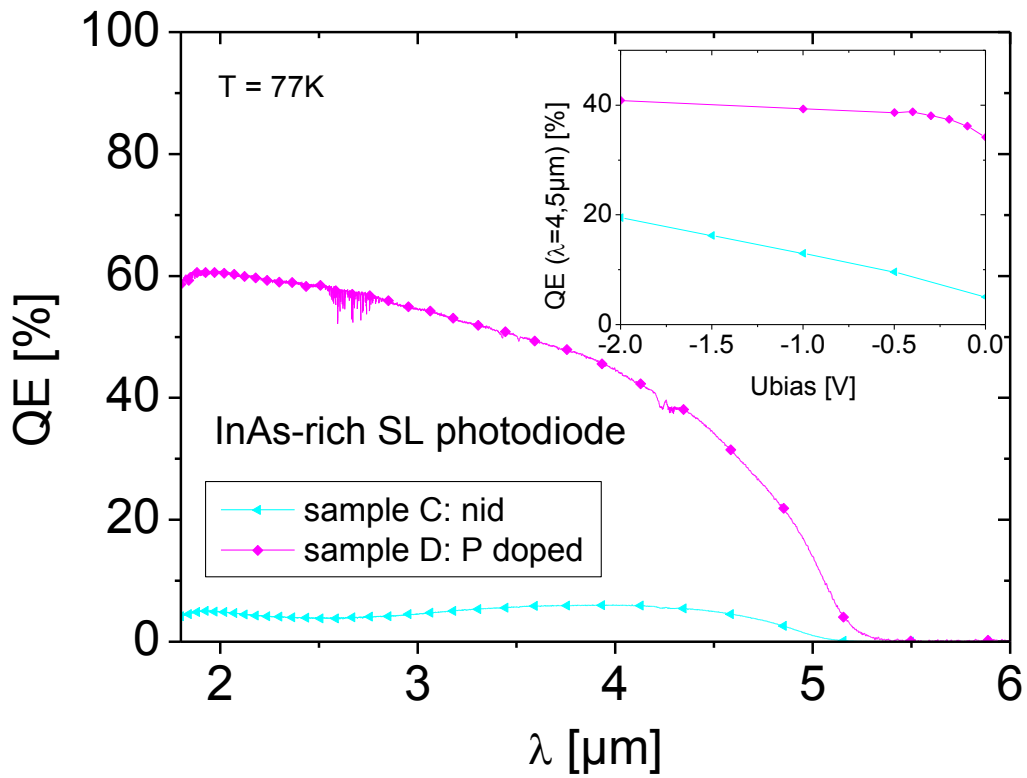
superlattice photodiodes

Figure 3

E. Giard *et al.*

Influence of the p-type doping on the radiometric performances of MWIR InAs/GaSb superlattice photodiodes
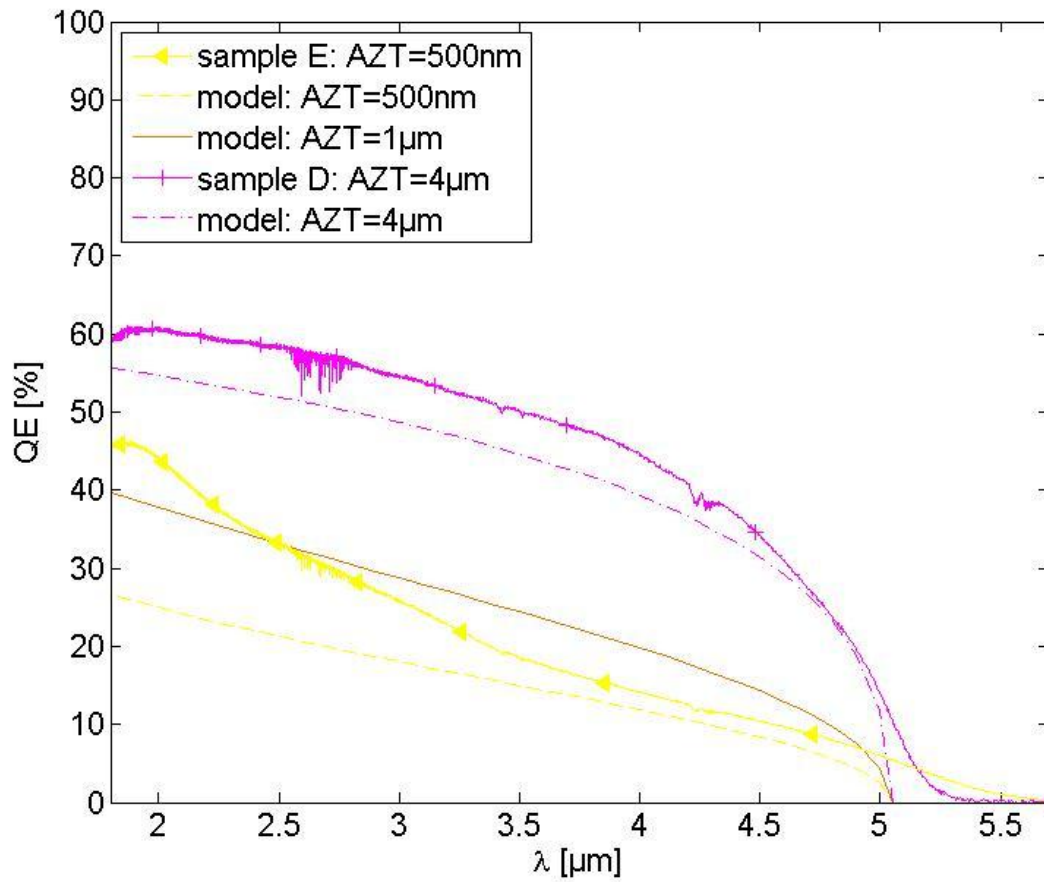
Figure 4

E. Giard *et al.*

Influence of the p-type doping on the radiometric performances of MWIR InAs/GaSb
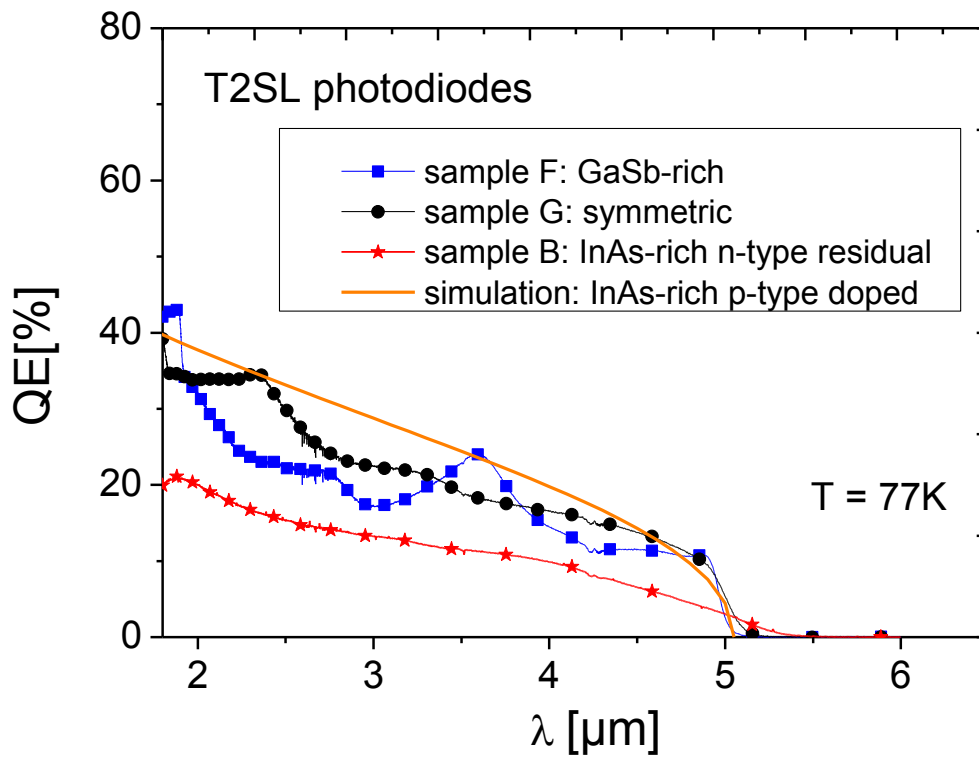
superlattice photodiodes

Figure 5

E. Giard *et al.*

Influence of the p-type doping on the radiometric performances of MWIR InAs/GaSb

superlattice photodiodes